NASA TECHNICAL MEMORANDUM 109043

Determination of Fiber-Matrix Interface Failure Parameters From Off-Axis Tests

Rajiv A. Naik and John H. Crews, Jr.

October 1993
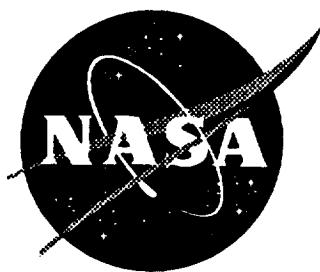
National Aeronautics and
Space Administration

LANGLEY RESEARCH CENTER
Hampton, Virginia 23681-0001

ABSTRACT

Critical fiber-matrix (FM) interface strength parameters were determined using a micromechanics-based approach together with failure data from off-axis tension (OAT) tests. The ply stresses at failure for a range of off-axis angles were used as input to a micromechanics analysis that was performed using the personal computer-based MICSTRAN code. FM interface stresses at the failure loads were calculated for both the square and the diamond array models. A simple procedure was developed to determine which array had the more severe FM interface stresses and the location of these critical stresses on the interface. For the cases analyzed, critical FM interface stresses were found to occur with the square array model and were located at a point where adjacent fibers were closest together. The critical FM interface stresses were used together with the Tsai-Wu failure theory to determine a failure criterion for the FM interface. This criterion was then used to predict the onset of ply cracking in angle-ply laminates for a range of laminate angles. Predictions for the onset of ply cracking in angle-ply laminates agreed with the test data trends.

INTRODUCTION

Damage-onset in polymer matrix laminated composite materials often initiates in the form of ply-cracks. Ply cracks often lead to delaminations or disbonds along the interfaces with neighboring plies [1, 2]. Under certain loading conditions, delaminations can lead to premature catastrophic failure. Ply cracking could also accelerate moisture absorption. From a design standpoint, it is, therefore, important to be able to predict the onset of ply cracking for critical components.

In the past, both macromechanical and micromechanical approaches have been used to predict the onset of ply cracking in a composite ply. Macromechanical failure theories such as the Tsai-Wu [3] tensor theory are commonly used along with ply-level stresses to predict ply failure under multiaxial stress states. Ply-level theories, however, do not provide any information about the mode of failure within the ply. Furthermore, ply strength parameters, determined for a given fiber volume fraction, cannot be used to predict failure in plies that have a different fiber volume fraction. A different set of strength parameters would have to be determined using appropriate ply testing for each fiber volume fraction of interest. Thus, ply level failure criteria that were established for a laminated ply with a 60% fiber volume fraction, for example, would not be directly applicable to predict yarn failure in a fabric reinforced composite, for example, with a 75% yarn fiber volume fraction.

For the prediction of ply cracking, if we assume that ply cracks result from a coalescence of micro-cracks that initiate at the fiber-matrix (FM) interface, then, ply cracking should be governed by critical stresses at the FM interface. A micromechanics based approach is required to calculate these critical FM interface stresses.

A micromechanical approach could potentially overcome both the shortcomings of the ply-level macromechanical approach. It could provide direct information about the mode of failure. Failures occurring in either the fibers, the matrix, or the fiber-matrix interface could be discerned. Also, since fiber volume fraction is a parameter in the micromechanics analysis, micromechanical strength parameters determined for a certain fiber volume fraction could be

2

directly used to predict the onset of cracking in a ply (or a yarn) with a different fiber volume fraction. Furthermore, a micromechanics analysis can also account for thermal and hygral stresses and, therefore, a single set of strength parameters could be used to predict ply cracking for a range of hygro-thermal conditions, thereby, significantly reducing the number of tests required to characterize ply cracking strength. Micromechanics-based strength parameters, determined from in-plane tests, also have the potential of being directly applicable to the prediction of composite strength under out-of-plane loading.

A micromechanics stress analysis, however, is generally more complicated than a ply-level stress analysis. Simplified micromechanics analyses have been used in the past for predicting ply failure. For example, Chamis [4, 5], Aboudi [6], and Sun [7] developed micromechanics analyses to calculate average stresses in sub-regions within the constituents. Simplified approaches often approximate circular fibers as square fibers [6, 7] and, therefore, lack the ability to calculate accurate stresses along the FM interface. Finite element analyses [8, 9, 10, 11] have often been used to overcome the shortcomings of the simplified approaches. However, due to its computer-intensive nature, a finite element analysis is not well suited for micromechanics-based failure prediction.

A micromechanics stress analysis, based on a classical elasticity solution [12, 13], that has the ability to model circular fibers with transversely isotropic properties arranged in either a square or a diamond array was developed recently by the authors [14]. Micromechanical FM interface stresses for various thermal and mechanical loadings were shown to be in excellent agreement with finite element results [14]. The analysis can be performed on a personal computer [15] and is, therefore, ideally suited for the development and also the application of micromechanics-based failure criteria.

The objective of the present study was to develop the basic concepts and procedures for a micromechanics-based technique to predict the onset of ply cracking in laminated composites or yarn splitting in textile composites. Ply cracking was assumed to be governed by critical stresses at the FM interface. Critical FM interface stresses were determined based on an

elastic micromechanics analysis together with unidirectional, off-axis tension test data for a range of FM interface stress states. These critical stresses were correlated using a form of the Tsai-Wu tensor theory, appropriate for FM interface failure, to determine critical FM interface strength parameters. These critical parameters were also used to predict the onset of ply cracking in angle-ply composites.

ANALYSIS

Within a composite ply, fibers are arranged randomly and may resemble a square array in some regions, a diamond array in some regions, and a hexagonal array in other regions. Micromechanics analyses usually assume that, within a ply, the fibers are arranged in a regular repeating array. The square, diamond, and hexagonal arrays are often used to calculate overall elastic constants and internal stresses in a composite ply. Under combined loading, the square and diamond array models have been shown [8] to produce higher stress concentrations than the hexagonal array model. The present study, therefore, used both the square and diamond array models to calculate critical FM interface stresses under thermal and mechanical loading conditions.

The micromechanics analysis for the square and diamond array models was developed earlier [14] and has been implemented in the personal computer based Micromechanical Combined Stress Analysis (MICSTRAN) [15] program. This analysis was based on a classical elasticity approach. Figure 1 shows the reference cylindrical (r-θ-z) and Cartesian (1-2-3) coordinate systems used in the analysis. The origin for both the models was located at the center of the fiber and the 1- and z-axes were oriented along the fiber direction. The 2-axis was constructed transverse to the fibers as shown, and the angle θ was measured from the 2-axis. As indicated by the shaded areas in Fig. 1, the analysis used the repeating unit cell ABCD for the square array and EGH for the diamond array .

The fibers were assumed to be circular in cross-section, homogeneous, and orthotropic with transverse isotropy in the 2-3 plane. The matrix was modelled as being homogeneous and

4

isotropic. The fiber and matrix were assumed to be perfectly bonded at the FM interface. A state of generalized plane strain was assumed (ε_1 = constant) for all loading cases except the longitudinal shear (σ_{12}) loading case. Details of the analysis procedures were presented in Ref. [14]. Only a brief outline of the overall procedure is included here.

The classical elasticity approach utilizing the Airy's stress function was used to analyze both the square and diamond array models. A general solution to the governing biharmonic equation was written in the form of a Fourier series, F, with arbitrary coefficients. The fiber and matrix regions were assigned a different set of arbitrary coefficients. The expressions for the stress components were determined from the stress function F by differentiation. The strain components were expressed in terms of the arbitrary coefficients by using the constitutive law. The expressions for the displacement components were obtained from the strain components by integration. Internal boundary conditions at the FM interface were used to satisfy stress equilibrium and displacement compatibility across the interface. These boundary conditions provided equations relating the arbitrary coefficients in the fiber and the matrix regions. External boundary conditions were satisfied at discrete points along the boundary, for each loading case, to determine the arbitrary coefficients by a point matching technique. This led to a truncation of the Fourier series and the accuracy of the computed FM interface stresses was verified by comparing with finite element solutions [14]. Results from the present analysis were in excellent agreement with the finite element results, for the square array model, [14] over a range of thermal and mechanical loading conditions. Results from the diamond array model are also expected to be accurate since the same stress function and procedure were used in the diamond array analysis.

Since the present study used an elastic analysis to calculate FM interface stresses, it was necessary to also check for matrix yielding. Matrix yielding was predicted using a Von Mises yield criterion [16] along with matrix stresses calculated using both the square and the diamond array models. Only those test cases for which specimen failure occurred before the onset of matrix yielding could be analyzed using the present elastic micromechanics analysis. Cases for

5

which matrix yielding preceded specimen failure were not considered in this study since they would require the use of an elasto-plastic micromechanics analysis.

TEST DATA

Off-axis tension (OAT) tests, for a range of off-axis angles, provide ply strength data for a range of ply stress states. Previously published test data [17] for the AS/3501-5A graphite/ epoxy composite material was used in the present study. Room temperature, dry conditions were reported for all the test cases that were analyzed here. Test specimens were 1.3 to 1.9 cm wide (with straight sides) and 7.5 to 12.7 cm long in the gage section. The final failure of the off-axis specimens was assumed to have occurred at the same load at which ply cracks initiated in the gage section. The ply stresses at failure (or at the onset of ply cracking) for the above tests are tabulated in Table I. These ply stresses were used as input to the micromechanics analysis to compute FM interface stresses at failure for each off-axis angle. Both the square and the diamond array models were used to compute these FM interface stresses.

PREDICTION OF THE ONSET OF PLY CRACKING

Although fibers are usually randomly arranged within a composite ply, the present study assumes that stresses computed using a regularly packed fiber array may be used to compute critical FM interface stresses. Within a composite ply, failure could initiate either in the matrix or at the FM interface. Under the combined action of shear and tensile normal stresses, it is assumed, that failure initiates at the FM interface and not in the matrix for two reasons: (i) the adhesive strength of the bond between the matrix and the fiber should be lower than the cohesive strength of the matrix, especially, under the action of tensile normal stresses, and (ii) the FM interface is subjected to higher stresses than the matrix. Furthermore, it was assumed that, for a high volume fraction polymer composite, FM interface failure at a critical point along the FM interface leads to a critical cross-sectional plane in the composite ply which

precipitates ply failure. Thus, ply stresses at the failure loads for off-axis tension tests were used to compute FM interface stresses that caused interface failure.

The FM interface is subjected to a combination of normal and shear stresses even under a uniaxial ply stress state [14]. Thus, to calculate critical FM interface strength parameters that characterize FM interface strength, it would be necessary to use an adhesive strength criterion that has been developed for such a combined state of stress. However, because such a strength criterion was not available, a phenomenological approach was necessary.

Two different approaches have been used for the evaluation of the bond strength between two different materials. The first approach uses an abrupt transfer model in which the properties of the two materials are assumed to be unchanged as they approach the interface and the interface is assumed to be a small contact layer (of negligible thickness) where intermolecular links exist between the two materials. The second approach uses a diffusion interlayer concept in which the contact between the two materials is made within a layer of finite thickness. The material properties of the diffusional contact layer are generally different from the two original materials. Uncertainties regarding the mechanical and strength properties of the diffusional layer usually limit the use of the latter approach.

The present study used the concepts of the abrupt transfer model [18] to compute the critical stresses at the FM interface that caused FM interface failure which led to the onset of ply cracking. The intermolecular links in the contact layer, for the abrupt transfer model, were assumed [18] to be broken only under tensile action. Such tensile action is possible only when normal tensile stresses, σ_{rr}, and, shear stresses, $\pm\sigma_{r\theta}$ and $\pm\sigma_{rz}$ are active either individually or simultaneously at the contact layer. Any other normal ($-\sigma_{rr}$, $\pm\sigma_{\theta\theta}$, $\pm\sigma_{zz}$) or shear ($\pm\sigma_{\theta z}$) stresses do not lead to a failure of the intermolecular links in the contact layer.

The only three stress components active along the FM interface are σ_{rr}, $\pm\sigma_{r\theta}$ and $\pm\sigma_{rz}$ [14]. At the failure load, these stresses combine, according to some physically admissible functional relationship, to become critical and contribute to the failure of the FM bond. This relationship between the normal and shear stresses constitutes a FM interface strength

criterion. The Tsai-Wu [3] tensor theory provides one such functional relationship. It is well suited to the prediction of FM interface failure since it can handle multi-axial stress states and allows for different strengths under tensile, compressive, and shear loading.

Using the three stress components that are active at the FM interface along with the assumption that the strength of the FM bond is infinite under compressive σ_{rr} stress, it was shown in [18] that the Tsai-Wu tensor theory for composite failure can be used to derive the following interface strength criterion:

$$\frac{\sigma_{rr}}{S_n} + \frac{\sigma_{r\theta}^2}{S_s^2} + \frac{\sigma_{rz}^2}{S_s^2} = 1 \tag{1}$$

where S_n is the FM interface strength normal to the interface and S_s is the shear strength of the FM interface. The shear strength, S_s, was assumed to be the same in the axial (z) and tangential (θ) directions. The combination of the σ_{rr}, $\pm\sigma_{r\theta}$ and $\pm\sigma_{rz}$ stresses at the FM interface which satisfies the interface strength criterion of Eqn. (1) will be referred to as critical FM interface stresses in the rest of this paper. Ply failure was assumed to initiate when stresses calculated for either the square or the diamond array combined to become critical at the FM interface.

Since the two shear stresses $\sigma_{r\theta}$ and σ_{rz} act on the same area at the FM interface (see Fig. 2), they can be combined as:

$$\tau_{eff} = \sqrt{\left(\sigma_{r\theta}^2 + \sigma_{rz}^2\right)} \tag{2}$$

where τ_{eff} is the effective shear stress acting at the FM interface. The interface strength criterion in Eqn. (1) can now be written as:

$$\frac{\sigma_{rr}}{S_n} + \frac{\tau_{eff}^2}{S_s^2} = 1 \qquad (3)$$

The FM interface strength criterion given by Eq. (3) was used in the present study. It was also useful to calculate a resultant stress, σ_{res}, at the FM interface by combining the normal stress, σ_{rr}, and the effective shear stress, τ_{eff}, as

$$\sigma_{res} = \sqrt{\left(\sigma_{rr}^2 + \tau_{eff}^2\right)} \qquad (4)$$

The strength parameters S_n and S_s in Eqn. (3) were determined by a three step procedure:

(i) FM interface stresses were calculated for each off-axis failure case using both the square and diamond array models in MICSTRAN.

(ii) Critical FM interface stresses σ_{rr} and τ_{eff} were determined for each test case by considering FM interface stresses for both the square and the diamond array models. Since the magnitudes and the locations of the peak σ_{rr}, $\pm\sigma_{r\theta}$ and $\pm\sigma_{rz}$ stresses at the FM interface were, in general, different for the square and the diamond array models a special procedure was used to determine the magnitude and location of the critical FM interface stresses and also the array which would be more critical at the failure load. For each failure case, the interface location and fiber array model with the largest resultant stress, σ_{res}, (see Eqn. (4) was assumed to be the the failure initiation site. The FM interface stresses at this location and for that fiber array were used as the critical FM interface stress values. Critical stresses were calculated, using this procedure, for each off-axis test case.

(iii) The calculated critical FM interface stresses, for a range of off-axis angles, were used together with Eqn. (3) in a regression analysis to determine the unknown strength parameters S_n and S_s.

RESULTS AND DISCUSSION

For the AS/3501-5A graphite/ epoxy composite, the thermo-mechanical properties for the 3501-5A epoxy matrix were not available. It was assumed that properties for the 3501-6 epoxy, made by the same manufacturer, would be similar to 3501-5A epoxy properties [19, 20] which are given in Table II. The longitudinal modulus for the AS fibers was available from the manufacturers data sheets [21]. Other fiber properties (see Table III) were estimated using a micromechanics analysis [15] from the properties of the matrix [19, 20] and the uni-directional composite [18]. A fiber volume fraction of 0.62 was used for all the analyses of the test data. The average ply stresses at failure (see Table I) were used as input to the micromechanics analysis for each test case. Thermal residual stresses due to cooldown from the curing temperature were computed by using $\Delta T = -100$ °C for all cases. These thermal residual stresses were superimposed with stresses due to mechanical loading to calculate FM interface and matrix stresses at failure.

In the following sections, test cases which may be analyzed using the present elastic analysis are identified. Next, the results for the FM interface stresses are presented for selected test cases. Then, critical FM interface stresses are presented for each test case and critical FM interface strength parameters are calculated. Finally, critical interface strength parameters are used to predict the onset of ply cracking in AS/3501-5A laminates having a range of ply angles.

Matrix Yielding

The matrix stresses at the FM interface for different combinations of applied normal stress, σ_{22}, and shear stress, σ_{12}, were calculated using both the square and diamond array models. These matrix stresses were used with the Von Mises yield criterion [16] and the matrix shear yield stress (Table II) to predict the applied stress level at which matrix yielding would occur at the FM interface. Figure 3 shows the predicted onset of matrix yielding. The

solid symbols in Fig. 3 indicate the off-axis tension strength [17] for the AS/3501-5A material for various off-axis angles, α. The shear dominated cases with $\alpha = 15$ and $\alpha = 30$ deg failed after the onset of matrix yielding. The normal stress dominated cases with $\alpha = 60$, 75, and, 90 deg failed before the onset of matrix yielding for both the square and the diamond array models. These cases may, therefore, be analyzed by an elastic micromechanics analysis. The $\alpha = 45$ deg case was a borderline case for which matrix yielding was predicted before failure using the square array model while the diamond array model did not predict any yielding. This case was also included in the present analysis for the determination of critical FM interface strength parameters. The $\alpha = 15$ and $\alpha = 30$ deg cases would require an elasto-plastic analysis to accurately compute the FM interface stresses at failure and were not analyzed using the present elastic analysis.

FM Interface Stresses

Figure 4 shows the stresses at the FM interface calculated using both the square and the diamond array models at the failure stress for the transverse tension ($\alpha = 90°$) test. In the absence of an applied longitudinal shear stress, the only stresses acting at the FM interface are the radial σ_{rr} stress and the shear $\sigma_{r\theta}$ stress. The peak radial stresses for both the arrays (after accounting for thermal residual stresses) occur at $\theta = 0°$ (*i.e.* where the fibers are closest together for the square array and farthest apart for the diamond array, see Fig. 1). The radial stress concentration factor (σ_{rr}/σ_{22}) for the square array is 1.1 which is about 10% higher than that for the diamond array. It was shown in Ref. [14] that the radial stress concentration is not sensitive to fiber volume fraction (or fiber spacing). The peak $\sigma_{r\theta}$ stress for the diamond array is -32.88 (located at $\theta = 40°$) which is about 27% higher than the square array peak located at $\theta = 60°$. The higher shear stresses lead to higher octahedral shear stresses and cause matrix yielding at lower applied σ_{22} stresses for the diamond array as compared to the square array (see Fig. 3).

The FM interface stresses at the failure stress for an off-axis angle $\alpha = 60$ deg are shown in Fig. 5. The σ_{rz} stress is active at the FM interface in addition to the σ_{rr} and $\sigma_{r\theta}$ stresses. In fact, these three stress components act at the FM interface for all OAT test cases, except, the transverse tension test case. For the $\alpha = 60$ deg case, the peak σ_{rr} and σ_{rz} stresses are almost equal for the square array model and occur at $\theta = 0°$. For the diamond array, the peak σ_{rr} stress occurs at $\theta = 0°$ and is 28% higher than the σ_{rz} peak stress which occurs at $\theta = 45°$. As for the transverse tension case, the peak $\sigma_{r\theta}$ stress for the diamond array is 27% higher than that for the square array. The three stress components shown in Fig. 5 combined to become critical at some point along the FM interface at failure. The location along the FM interface where the stresses would become critical is not obvious. Furthermore, it is also not clear which array would be more critical at the failure stress.

Critical FM Interface Stresses and Strength Parameters

The location of the critical FM interface stresses and the array which produced the more critical stresses were determined by calculating the resultant interface stress σ_{res} as described earlier (see Eqs. (2) and (4)). Figure 6 shows the σ_{res} stress around the FM interface calculated for the $\alpha = 60$ deg case using both the square and diamond array models. Although the σ_{res} stress for the diamond array is higher in the $\theta = 30°\text{-}70°$ region, the peak σ_{res} stress occurs at the $\theta = 0°$ location for the square array. Thus for the $\alpha = 60$ deg case, the critical FM interface stresses occurred at $\theta = 0°$ and the square array was more critical than the diamond array. This procedure was repeated for the other OAT test cases.

Figure 7 shows the critical stresses for all the OAT test cases analyzed in this study on a $\sigma_{rr} - \tau_{eff}$ plot. The effective shear stress, τ_{eff}, at the FM interface was calculated by combining the shear stress components acting on the interface (see Eq. (2)). Based on the critical FM interface stresses in Fig. 7, it is clear that OAT tests can be used to induce a wide range of critical stress states at the FM interface. For all the cases analyzed, the critical stresses occurred at the $\theta = 0°$ location and the square array model was more critical in each

case. These critical stresses were used in the computation of critical FM interface strength parameters which are required in the interface strength criterion of Eq. (3).

As described earlier, the critical strength parameters S_n and S_s (see Eq. (3)) were determined by using the critical FM interface stresses in Fig. 7 along with Eq. (3) in a regression analysis. Figure 8 shows the critical FM interface stresses along with the calculated strength parameters S_n and S_s and a plot of Eq. (3) using these strength parameters. Equation (3) correlates well with the critical stresses computed from OAT failure data and provides a means to predict FM interface failure over the range of stress states shown in Fig. 8.

It is important to note that the application of Eq. (3) has been demonstrated in the present study only for combinations of longitudinal shear and *tensile* normal stresses that occur in OAT tests. For ply stress states that involve combinations of longitudinal shear and *compressive* normal stresses, ply cracking may not initiate as a result of FM interface failure and a different failure criterion may be required.

Prediction of Ply Cracking Strength for Angle-Ply Laminates

The critical interface strength parameters S_n and S_s were used together with Eq. (3) to predict the onset of ply cracking in angle-ply laminates made of AS/3501-5A over a range of ply angles. An incremental load approach was used in the prediction of ply cracking. At each load increment, classical lamination theory (CLT) was used to compute stresses in each off-axis ply. CLT was also used to compute thermal residual stresses in each ply. The resultant (mechanical + thermal) stresses were then applied to the micromechanics models. MICSTRAN was used to compute FM interface stresses. The σ_{res} procedure, described earlier, was then used to determine the fiber array with the critical FM interface stresses. Ply cracking was predicted for the load at which the calculated FM interface stresses, for the critical fiber array, satisfied the failure criterion of Eqn. (3) at some interfacial location.

Figure 9 shows the predictions for the onset of ply cracking over a range of ply angles. Tension strength data [17] for the AS/3501-5A material, for the $\pm$75 deg and the $\pm$60 deg laminates are also shown in Fig. 9. The prediction and experimental data for the transverse tension test, shown earlier in Fig. 8, is also plotted in Fig. 9. The predicted increase in ply cracking strength with decreasing laminate angle is consistent with the test data. Note that the data corresponds to ultimate failure while the predictions are for the onset of ply cracking. For the 90 deg and $\pm$75 deg laminates the onset of ply cracking and ultimate failure probably occurred in quick succession, however, for the $\pm$60 deg laminate ply cracking could have led to the progression of delamination before final failure occurred. Further testing is required to fully verify the predictions in Fig. 9.

SUMMARY

Critical fiber-matrix (FM) interface strength parameters were determined using a micromechanics-based approach together with test data from off-axis tension (OAT) tests. OAT test data for the AS/3501-5A material system were used. The ply stresses at failure for a range of off-axis angles were used as input to a micromechanics analysis that was performed using the personal computer-based MICSTRAN program. The FM interface stresses at the failure loads were calculated for both the square and the diamond array models. Test cases for which failure preceded matrix yielding were analyzed using the present elastic analysis. A simple procedure was developed to determine the locations of the critical FM interface stresses and the critical fiber array for each OAT test case. The critical FM interface stresses were used together with the Tsai-Wu failure theory to determine critical parameters at the FM interface. These critical parameters were then used to predict the onset of ply cracking in angle-ply laminates for a range of laminate angles.

Analysis results indicated that OAT tests could be used to induce a wide range of stress states at the FM interface. The magnitudes and locations of the peak stresses computed using the square and the diamond array models were quite different. The square array led to higher

normal and longitudinal shear stresses while the diamond array usually led to higher transverse shear stresses at the FM interface.

For the cases analyzed, critical FM interface stresses were found using the square array model and were located at a point where adjacent fibers were closest together. The Tsai-Wu failure theory, applied at the FM interface, provided a good correlation with test data. Predictions for the onset of ply cracking in angle-ply laminates made using the present micromechanics-based critical strength parameters followed the trends in the test data but need further verification.

REFERENCES

1. Crossman, F. W. and Wang, A. S. D.: "The Dependence of Transverse Cracking and Delamination on Ply Thickness in Graphite/Epoxy Laminates," *Damage in Composite Materials, ASTM STP 775,* American Society for Testing and Materials, Philadelphia, 1982, pp. 118-139.

2. Reifsnider, K. L. and Talug, A.: "Analysis of Fatigue Damage in Composite Laminates," *International Journal of Fatigue,* Vol. 3, No. 1, Jan. 1980, pp. 3-11.

3. Tsai, S. W. and Wu, E. M.: "A General Theory of Strength for Anisotropic Materials," *J. Comp. Mater.,* Vol. 5, Jan. 1971, pp. 58-80.

4. Chamis, C. C.: "Simplified Composite Micromechanics for Predicting Microstresses," *J. Reinforced Plastics and Composites,* Vol. 6, July 1987, pp. 268-289.

5. Chamis, C. C.: "Simplified Composite Micromechanics Equations for Strength, Fracture Toughness, and Environmental Effects," *SAMPE Q.,* Vol. 15, No. 4, July 1984, pp. 41-55.

6. Aboudi, J.: "Micromechanical Analysis of the Strength of Unidirectional Fiber Composites," *Comp. Sci. Technol.,* Vol. 33, 1988, pp. 79-96.

7. Sun, C. T.: "Modeling Continuous Fiber Metal Matrix Composite as an Orthotropic Elastic-Plastic Material," *Metal Matrix Composites: Testing, Analysis and Failure Modes, ASTM STP 1032,* W. S. Johnson, Ed., American Society for Testing and Materials, Philadelphia, 1989, pp. 148-160.

8. Foye, R. L.: "An Evaluation of Various Engineering Estimates of the Transverse Properties of Unidirectional Composites," *Proc. 10th Nat. Symp., Soc. Aerosp. Mater. Process Eng.,* San Diego, Calif., Nov. 9-11, 1966, pp. G-31 to G-42.

9. Bigelow, C. A., Johnson, W. S., and Naik, R. A.: "An Comparison of Various Micromechanics Models for Metal Matrix Composites, Mechanics of Composite Materials and Structures, Eds. J. N. Reddy and J. L. Teply, Book No. HOO464 - 1989, pp. 21-31, The American Society of Mechanical Engineers.

10. Wisnom, M. R.: "Factors Affecting the Transverse Tensile Strength of Unidirectional Continuous Silicon Carbide Fibre Reinforced 6061 Aluminum," *J. Comp. Mater.*, Vol. 24, No. 7, July 1990, pp. 707-726.

11. Nimmer, R. P., Bankert, R. J., Russell, E. S., Smith, G. A., and Wright, P. K.: "Micromechanical Modeling of Fiber/ Matrix Interface Effects in Transversely Loaded SiC/Ti-6-4 Metal Matrix Composites, *J. Comp. Tech. & Res.*, Vol. 13, No. 1, Spring 1991, pp. 3-13.

12. Kobayashi, S. and Ishikawa, T.: "Elastic Properties of Unidirectional Fiber-Reinforced Composites," *Fukugo Zairyo Kenkyu (Composite Materials and Structures)*, Vol. 3, No. 3, 1974, pp. 12-20.

13. Ishikawa, T. and Kobayashi, S.: "Elastic Properties of Unidirectional Fiber-Reinforced Composites II," *Fukugo Zairyo Kenkyu (Composite Materials and Structures)*, Vol. 3, No. 4, 1974, pp. 23-31.

14. Naik, R. A. and Crews, J. H. Jr.: "Closed-Form Analysis of Fiber-Matrix Interface Stresses Under Thermo-Mechanical Loadings," NASA TM-107575, Mar. 1992, National Aeronautics and Space Administration, Hampton, Virginia.

15. Naik, R. A.: "Micromechanical Combined Stress Analysis - MICSTRAN, A User Manual," NASA CR-189694, Oct. 1992, National Aeronautics and Space Administration, Hampton, Virginia.

16. Mendelson, A.: *Plasticity Theory and Application*, Robert E. Krieger Publishing Company, Malabar, Florida, 1983.

17. Kim, R. Y.: "On the Off-Axis and Angle-Ply Strength of Composites," *Test Methods and Design Allowables for Fibrous Composites, ASTM STP 734*, C. C. Chamis, Ed., American Society for Testing and Materials, 1981, pp. 91-108.

18. Skudra, A. M.: "Micromechanics of Failure of Reinforced Plastics," Chapter 1, *Handbook of Composites*, Vol. 3 - Failure Mechanics of Composites, Eds., G. C. Sih and A. M. Skudra, 1985, Elsevier Science Publishers B. V., pp. 1-69.

19. Adams, D. F. and Schaffer, B. G.: "Analytical/Experimental Correlations of Stiffness Properties of Unidirectional Composites," *Composites Technol. Rev.,* Vol. 4, No. 2, Summer 1982, pp. 45-48.

20. Adams, D. F.: "A Micromechanics Analysis of the Influence of the Interface on the Performance of Polymer-Matrix Composites," *Jl. Reinforced Plastics and Composites,* Vol. 6, Jan. 1987, pp. 66-88.

21. "Hercules Magnamite Graphite Fibers," Hercules, Inc., Magna, Utah, 1978.

Table I.- Ply stresses at failure for off-axis tension (OAT) tests [17].

Fiber angle, deg.	σ_{11}, MPa	σ_{22}, MPa	σ_{12}, MPa
90	0.0	51.7	0.0
75	4.1	56.7	15.2
60	18.0	54.1	31.2
45	45.5	45.5	45.5
30	101.4	33.8	58.5
15	288.0	20.7	77.3

Table II.- Thermo-mechanical properties for 3501-6 epoxy [19,20]

E, GPa	ν	CTE (10^{-6}/ °C)	Shear yield stress, MPa
4.3	0.34	40.0	56.3

Table III.- Estimated thermo-mechanical properties of AS fibers.

E_{11}, GPa	E_{22}, GPa	ν_{12}, ν_{13}	ν_{23}	G_{12}, G_{13}, GPa	G_{23}, GPa	$(CTE)_{11}$ (10^{-6}/ °C)	$(CTE)_{22}$ (10^{-6}/ °C)
220.0 [Ref. 21]	14.0	0.25	0.27	60.0	5.5	-0.6	15.0
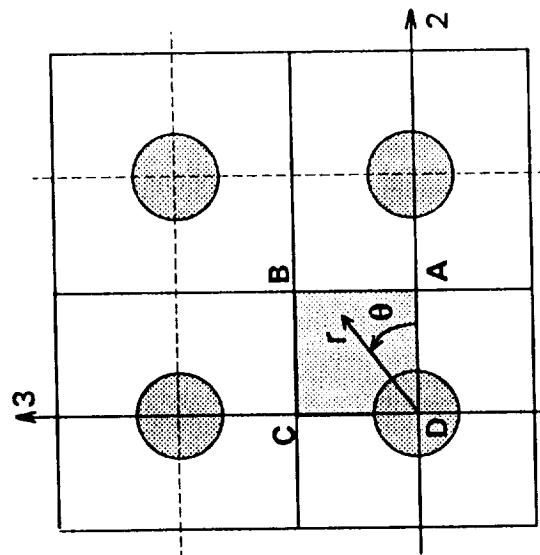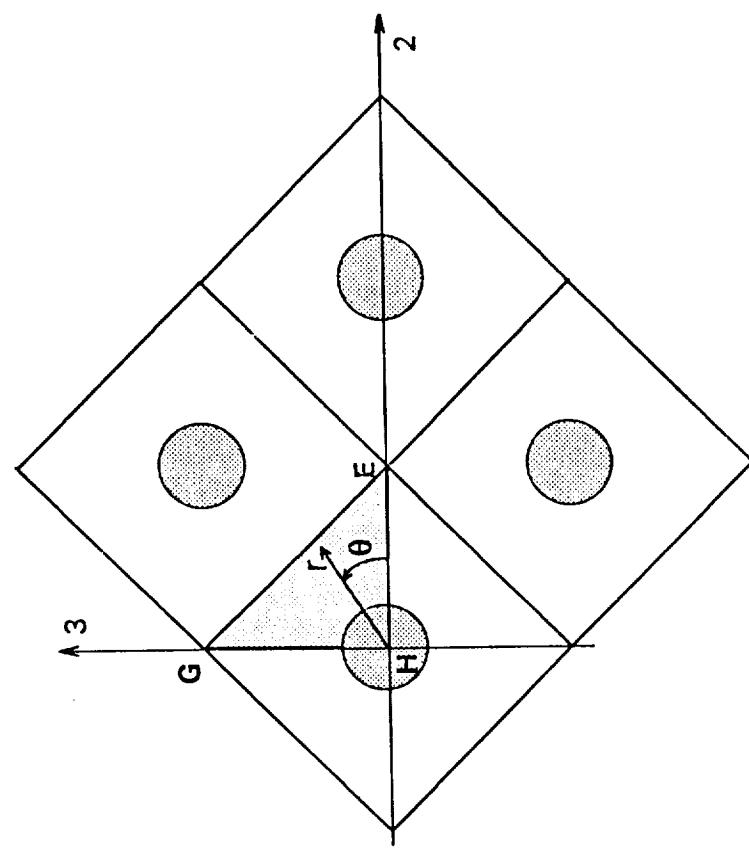
Fig. 1.- Configurations for the square and diamond array models.
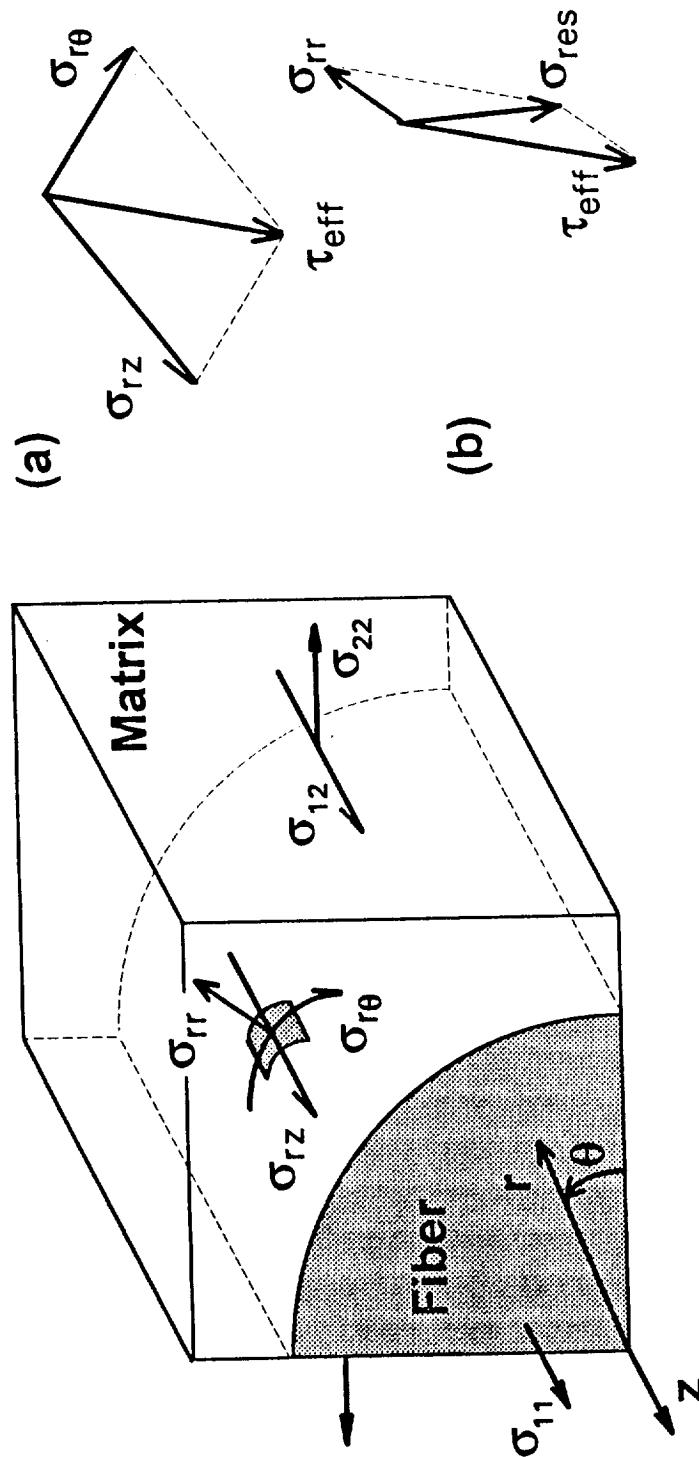
Fig. 2. - Effective shear stress (τ_{eff}) and resultant interface stress (σ_{res}) at fiber-matrix interface.
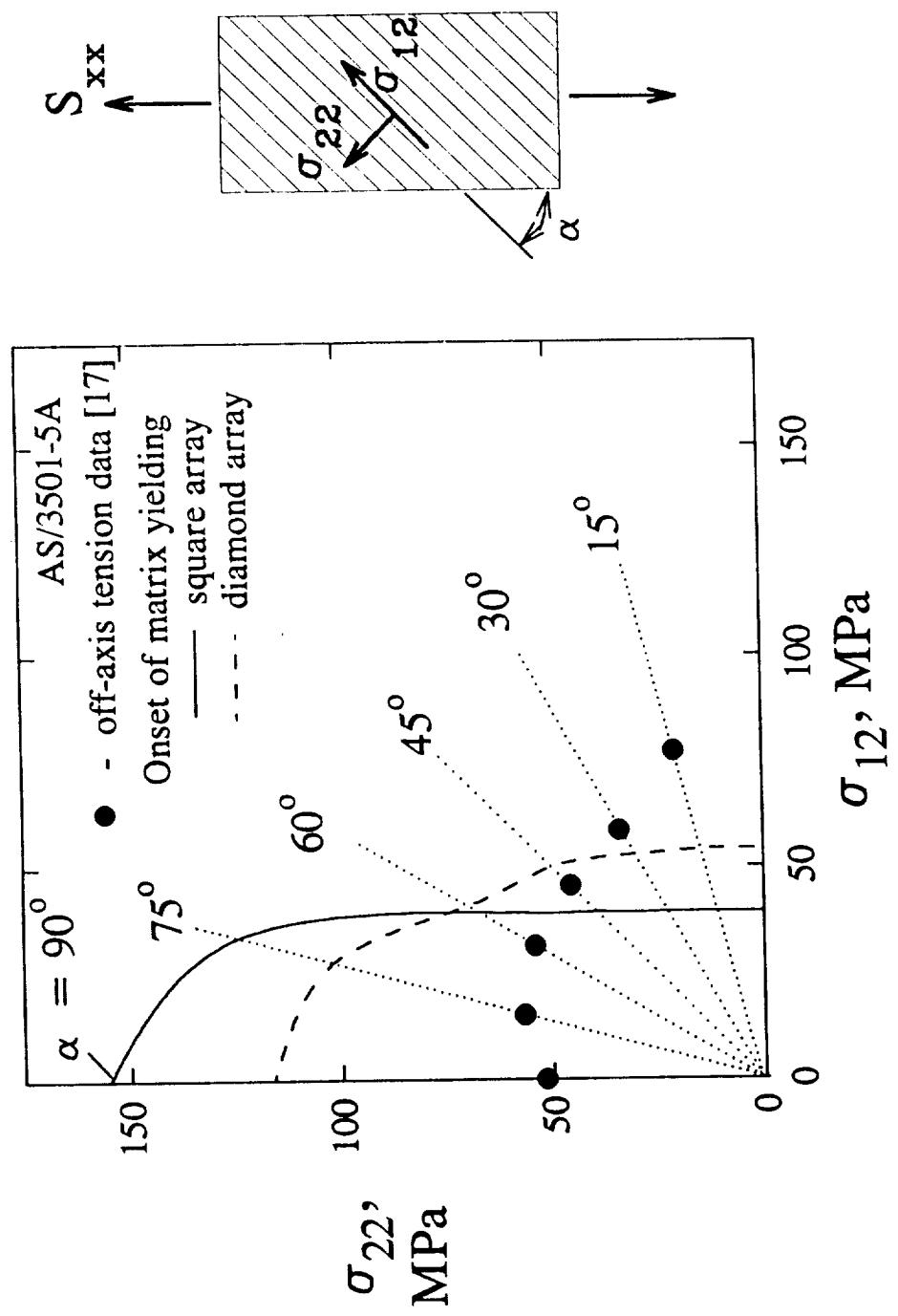
Fig. 3. - Off-axis tension failure data and calculated matrix yield curves.

Ply stresses: $\sigma_{11} = 0$, $\sigma_{22} = 51.7$ MPa, $\sigma_{12} = 0$
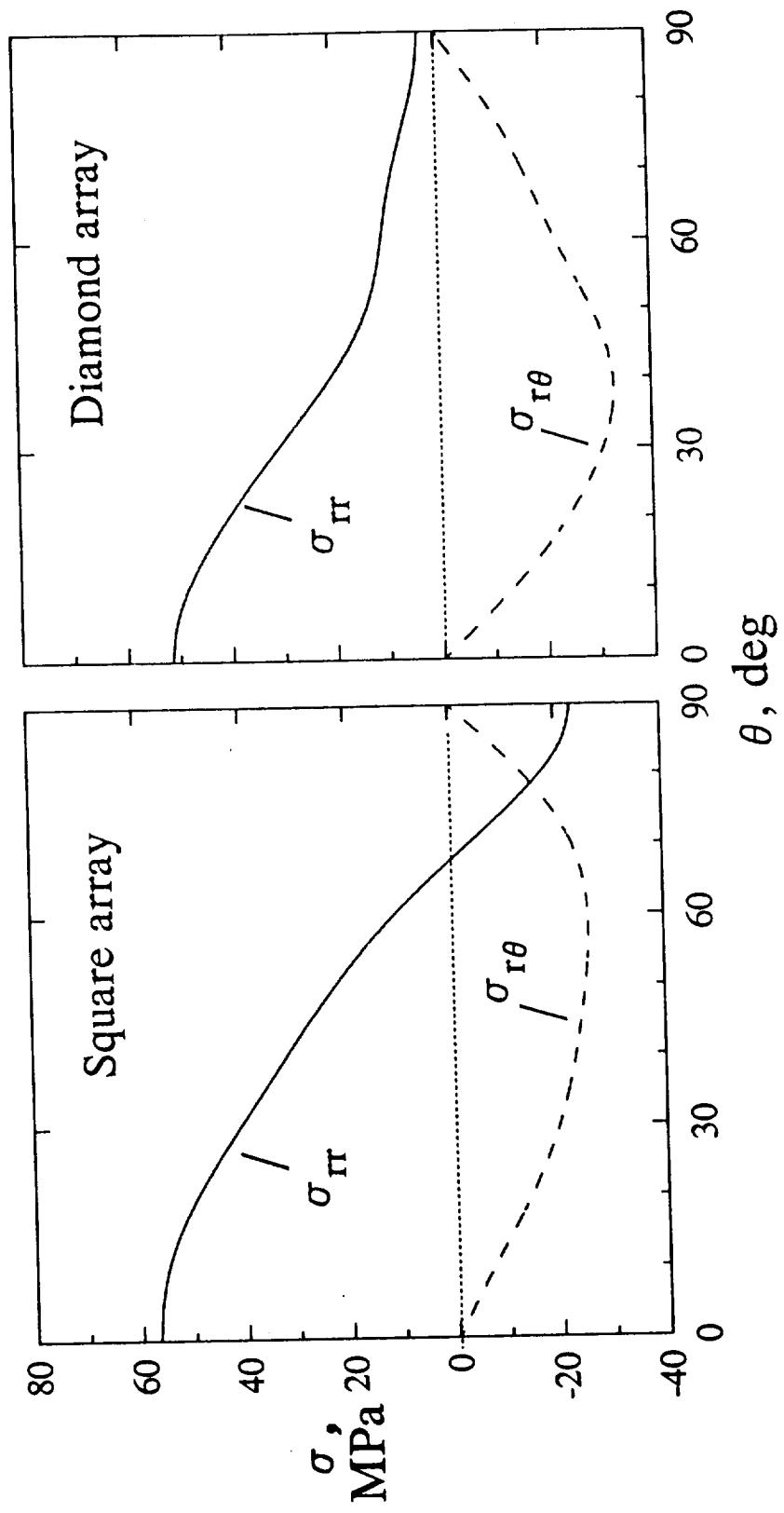
Fig. 4. - Fiber-matrix interface stresses (using MICSTRAN) at failure for transverse tension test.

Ply stresses: $\sigma_{11} = 18.0$ MPa, $\sigma_{22} = 54.1$ MPa, $\sigma_{12} = 31.2$ MPa
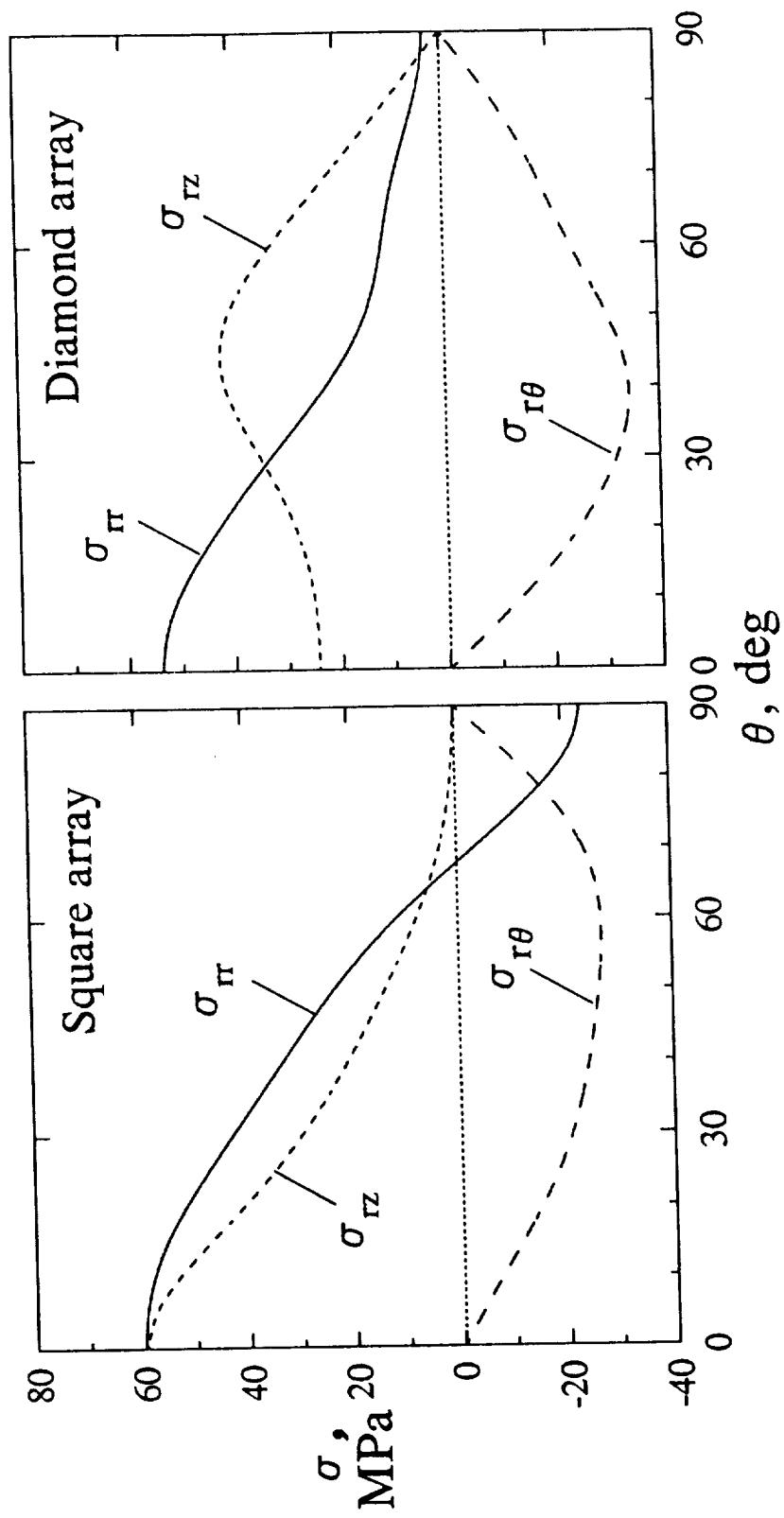
Fig. 5. - Fiber-matrix interface stresses (using MICSTRAN) at failure for the 60 deg OAT test.
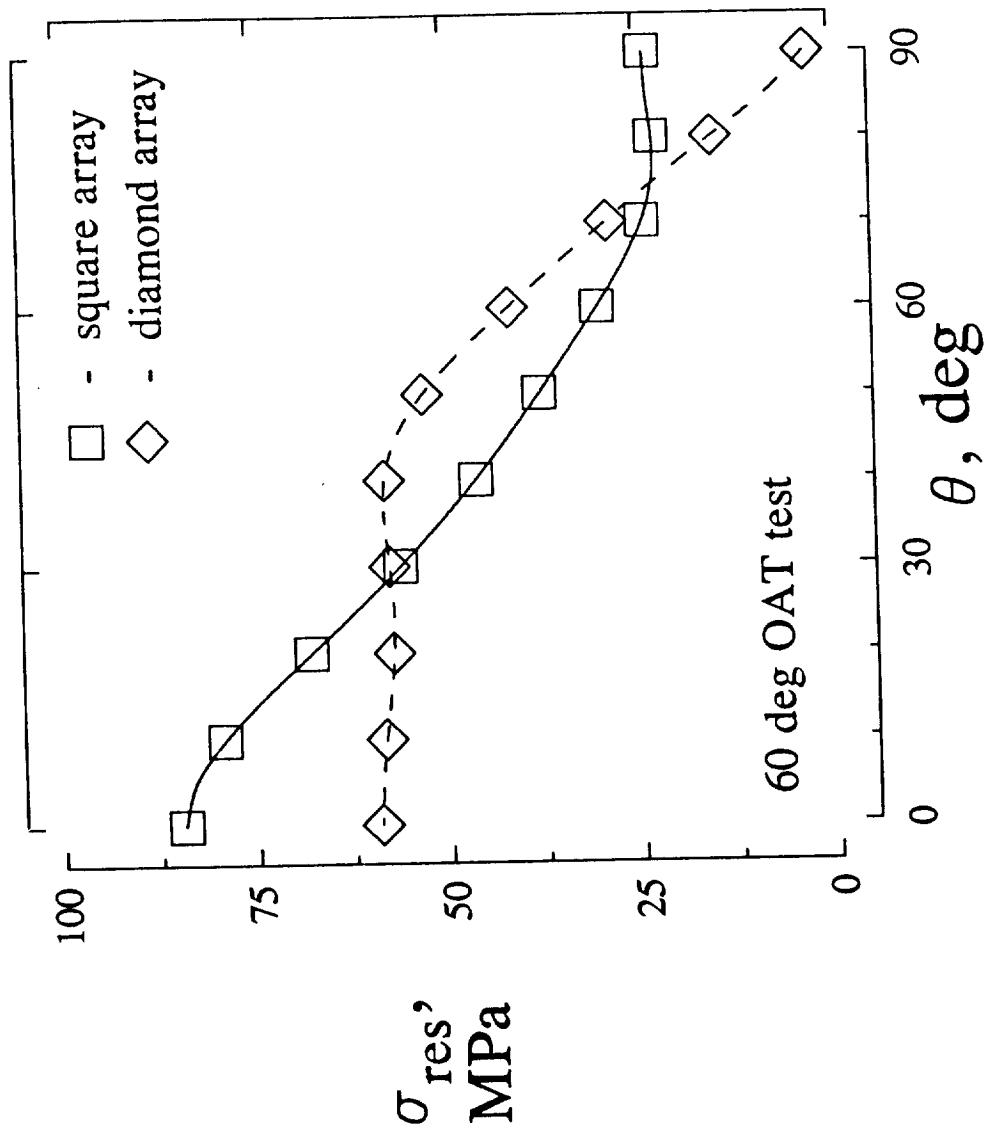
Fig. 6. - Variation of σ_{res} (Eqn. (4)) around fiber-matrix interface for 60 deg OAT test.

25
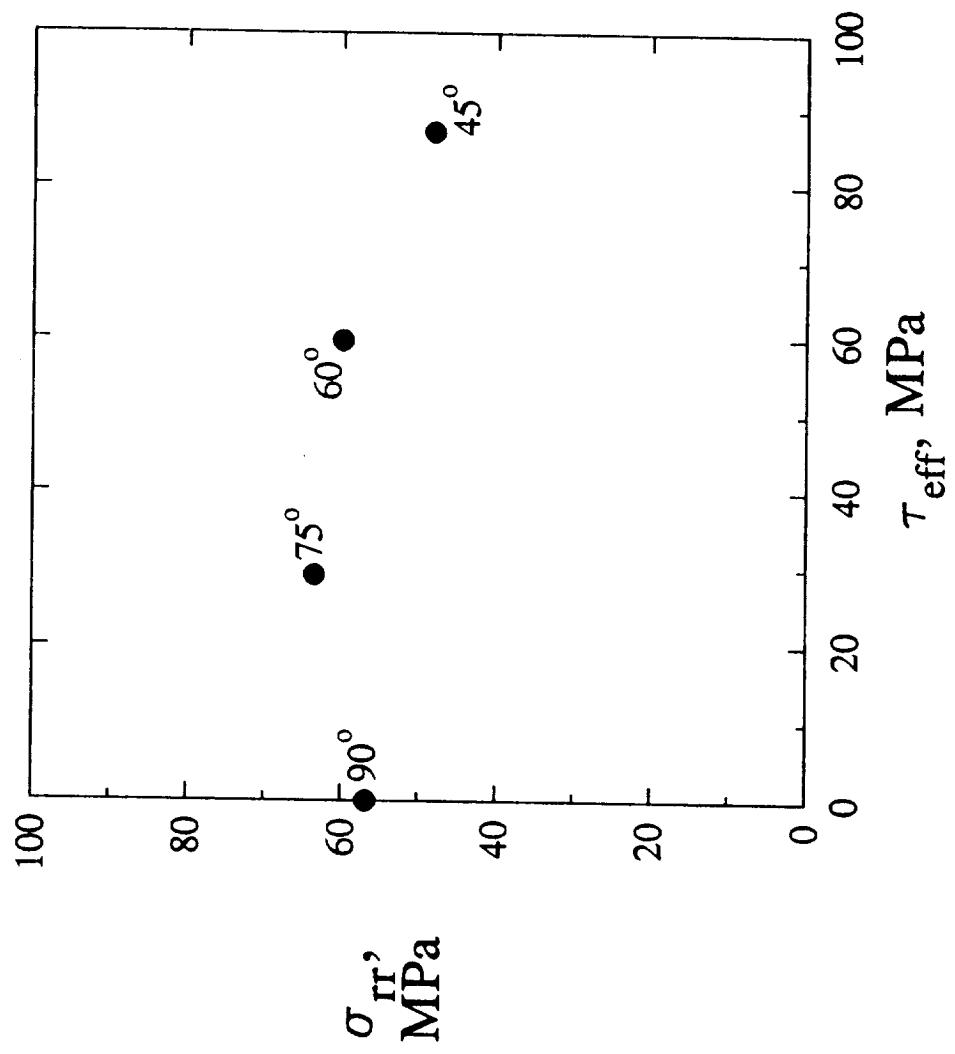
Fig. 7. - Critical fiber-matrix interface stresses at failure for OAT tests.
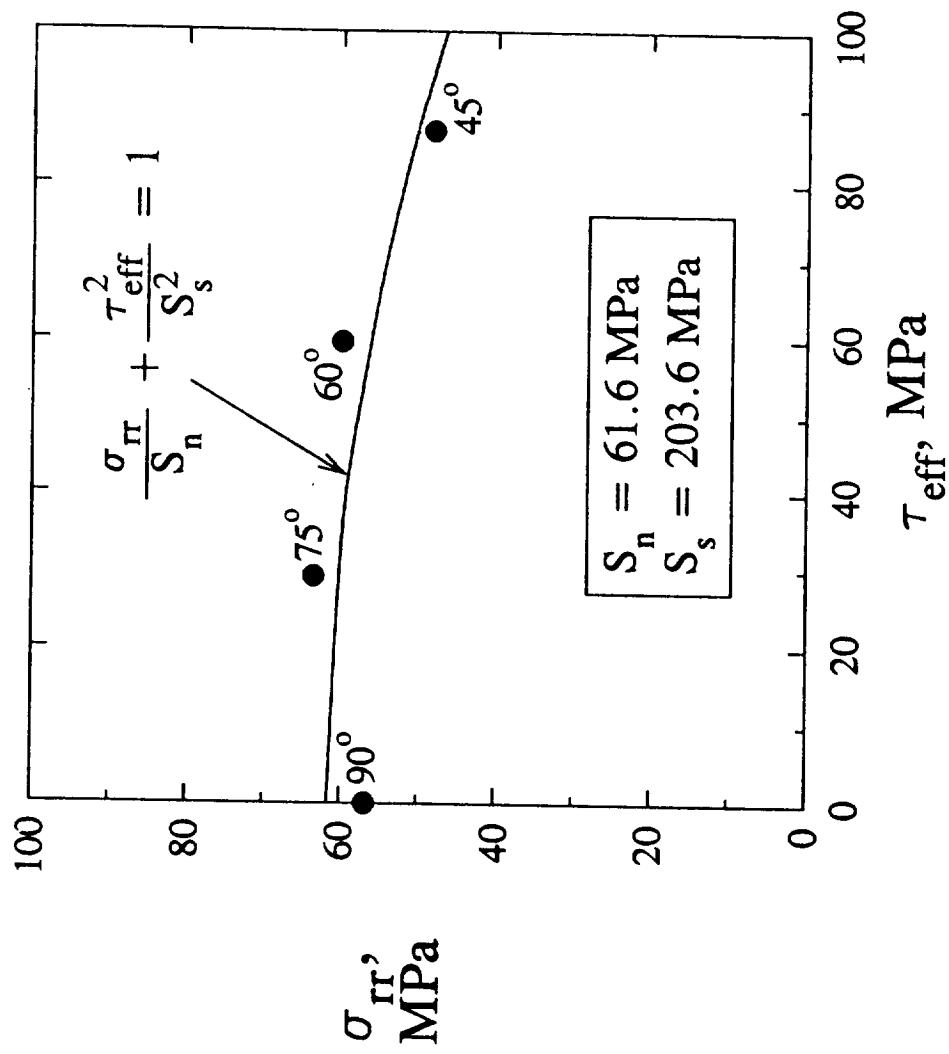
Fig. 8. - Regression fit using Eq. (3) for a range of off-axis angles.

27
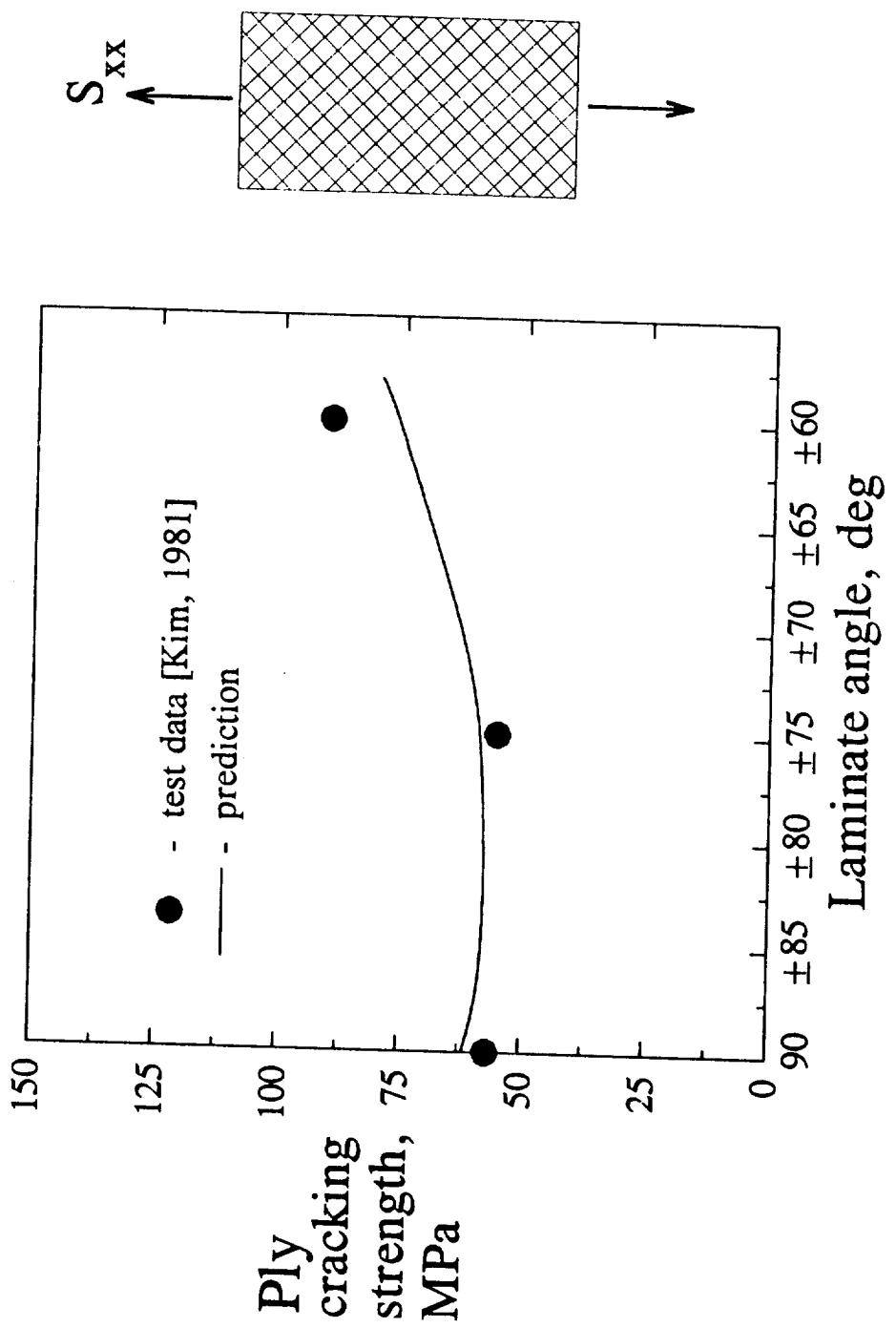
Fig. 9. - Prediction of ply cracking onset for angle-ply laminates.

REPORT DOCUMENTATION PAGE

Public reporting burden for this collection of information is estimated to average 1 hour per response, including the time for reviewing instructions, searching existing data sources, gathering and maintaining the data needed, and completing and reviewing the collection of information. Send comments regarding this burden estimate or any other aspect of this collection of information, including suggestions for reducing this burden, to Washington Headquarters Services, Directorate for Information Operations and Reports, 1215 Jefferson Davis Highway, Suite 1204, Arlington, VA 22202-4302, and to the Office of Management and Budget, Paperwork Reduction Project (0704-0188), Washington, DC 20503

1. AGENCY USE ONLY (Leave blank)	2. REPORT DATE October 1993	3. REPORT TYPE AND DATES COVERED Technical Memorandum

4. TITLE AND SUBTITLE Determination of Fiber-Matrix Interface Failure Parameters From Off-Axis Tests	5. FUNDING NUMBERS WU 505-63-50-04

6. AUTHOR(S)

Rajiv A. Naik and John H. Crews, Jr.

7. PERFORMING ORGANIZATION NAME(S) AND ADDRESS(ES) NASA Langley Research Center Hampton, VA 23681-0001	8. PERFORMING ORGANIZATION REPORT NUMBER

9. SPONSORING / MONITORING AGENCY NAME(S) AND ADDRESS(ES) National Aeronautics and Space Administration Washington, DC 20546-0001	10. SPONSORING / MONITORING AGENCY REPORT NUMBER NASA TM 109043

11. SUPPLEMENTARY NOTES

Naik: Analytical Services & Materials, Inc., Hampton, VA
Crews: Langley Research Center, Hampton, VA

12a. DISTRIBUTION / AVAILABILITY STATEMENT Unclassified - Unlimited Subject Category - 26	12b. DISTRIBUTION CODE

13. ABSTRACT (Maximum 200 words)

Critical fiber-matrix (FM) interface strength parameters were determined using a micromechanics-based approach together with failure data from off-axis (OAT) tests. The ply stresses at failure for a range of off-axis angles were used as input to a micromechanics analysis that was performed using the personal computer-based MICSTRAN code. FM interface stresses at the failure loads were calculated for both the square and the diamond array models. A simple procedure was developed to determine which array had the more severe FM interface stresses and the location of these critical stresses on the interface. For the cases analyzed, critical FM interface stresses were found to occur with the square array model and were located at a point where adjacent fibers were closest together. The critical FM interface stresses were used together with the Tsai-Wu failure theory to determine a failure criterion for the FM interface. This criterion was then used to predict the onset of ply cracking in angle-ply laminates for a range of laminate angles. Predictions for the onset of ply cracking in angle-ply laminates agreed with the test data trends.

14. SUBJECT TERMS Ply cracking; Interface strength; Failure criterion; Composite laminate; Micromechanics; Damage onset	15. NUMBER OF PAGES 29
	16. PRICE CODE A03

17. SECURITY CLASSIFICATION OF REPORT Unclassified	18. SECURITY CLASSIFICATION OF THIS PAGE Unclassified	19. SECURITY CLASSIFICATION OF ABSTRACT	20. LIMITATION OF ABSTRACT